Supporting Information for

Inhibiting grain coarsening and inducing oxygen vacancy: the roles of Mn in achieving highly reversible conversion reaction and long life SnO_2-Mn-graphite ternary anode

*Renzong Hu, Yunpeng Ouyang, Tao Liang, Xin Tang, Bin Yuan, Jun Liu, Lei Zhang, Lichun Yang, and Min Zhu**

Prof. R. Hu, Y. Ouyang, T. Liang, Prof. B. Yuan, Prof. J. Liu, Dr. L. Yang, and Prof. M. Zhu

Guangdong Provincial Key Laboratory of Advanced Energy Storage Materials, School of Materials Science and Engineering, South China University of Technology, Guangzhou, 510640, China
*E-mail: memzhu@scut.edu.cn

Prof. X. Tang

Department of Material and Chemical Engineering, Guilin University of Technology, Guilin 541004, China

Prof. L. Zhang

School of Chemistry and Chemical Engineering, South China University of Technology, Guangzhou, 510640, China

Note 1 Calculations of the formation energy of oxygen vacancy in SnO_2 and Mn-doped SnO_2

The calculations were performed in the framework of DFT with the projected augmented wave (PAW) method [1], using the Vienna *ab initio* simulation package (VASP) [2,3], which is effective in describing the crystal and electronic structure of the condensed matter. For the exchange-correlation functional, a spin-polarized generalized gradient approximation (GGA) [4] in the form of Perdew-Burke-Ernzerhof (PBE) is employed. For valence electrons, the outermost s and d states of Mn atoms, s and p states of O and Sn atoms are employed in the work. Previous first principle calculation [5] has shown that Mn dopants in SnO_2 favor a spin polarization. So, spin GGA is applied when Mn atom appears in supercell. The plane-wave energy cutoff is set to 400 eV and a Γ-point centered 3×3×3 k-point mesh is used to sample the supercell, which consists of 72 atoms with 24 Sn atoms and 48 O atoms.

In order to describe the formation energy and the transition energy, we follow the procedure in Ref.[6-8], which has been used successfully for studying defects in various semiconductors. The formation energies of the defects are given by:

$$\Delta E_f(\alpha) = E(\alpha) - E(host) + \sum_i n_i(E(i) + \mu_i) \quad (1)$$

where $E(\alpha)$ and E(host) are the total energy of the supercell with and without the defect α. n_i indicates the number of atoms of type i (host atoms or impurity atoms) that have been added to ($n_i < 0$) or removed from ($n_i > 0$) the supercell. μ_i is the chemical potential of constituent i referenced to elemental solid/gas with formation energy of $E(i)$. μ_{Sn} and μ_O obey the equilibrium condition $\mu_{Sn} + 2\mu_O = \Delta H_f(SnO_2) = -5.09$ eV, where $\Delta H_f(SnO_2)$ is the calculated formation energy of SnO_2, compared to the experimental value of -5.94 eV [9]. In order to avoid the formation of the secondary phases, μ_{Sn}, μ_O and μ_{Mn} must satisfy the following conditions:

$\mu_{Mn} + 2\,\mu_O \le \Delta H_f(MnO_2)$;
$\mu_{Mn} + \mu_O \le \Delta H_f(MnO)$;
$\mu_{Mn} \le \mu(Mn, bulk) = 0$ eV;
$\mu_{Sn} \le \mu(Sn, bulk) = 0$ eV;
$\mu_O \le \mu(O_2, gas) = 0$ eV

ΔH_f represents the formation enthalpy of the secondary phases. The calculated and experimental values are listed in **Table S1**. Since O vacancies (V_O) often form under Sn-rich condition ($\mu_O = -2.55$eV, $\mu_{Sn} = 0$ eV), the following calculation is focused on the condition. **Table S2** is the formation energies of the main defects in SnO_2. The result shows that the V_O-Mn_{Sn} complex is 0.94 eV lower than the single V_O in formation energy, which also means Mn_{Sn} favors the formation V_O.

Table S1 The cohesive energies and the formation energies of the possible secondary phases in Mn doped SnO_2. The values in parenthesis are the experimental data from Ref. 9

Secondary phase / Element	Cohesive energy (eV)	Formation energy (eV)
Sn,bulk	-3.05 (-3.05[a])	
Mn,bulk	-3.89 (-2.28 [a])	
$O(O_2,gas)$	-3.25 (-2.58 [a])	
MnO_2		-4.85 (-5.36[a])
MnO		-2.46 (-3.96 [a])

[a] Reference 9

Table S2 The formation energies of V_O, Mn_{Sn}, and V_O-Mn_{Sn} in SnO_2 under Sn-rich condition.

Defects	Formation energy (eV)
V_O	2.97
Mn_{Sn}	-3.56
V_O-Mn_{Sn}	2.03

Reference S

[1] G.Kresse and D.Joubert, Phys. Rev. B **59** (1999) 1758
[2] G.Kresse and J.Furthmuller, Comput. Mater. Sci. **6** (1996) 15
[3] G.Kresse and J.Furthmuller, Phys. Rev. B **54** (1996) 11169
[4] J.P. Perdew, Y. Wang, Physical Review B, 45 (1992) 13244-13249.
[5] X L Wang, Z X Dai and Z Zeng, J. Phys.: Condens. Matter 20 (2008) 045214
[6] Y. Yan and S.H. Wei, Phys. Status Solidi B 245 (2008) 641
[7] S.H. Wei, Comput. Mater. Sci. **30** (2004) 337
[8] R.Y. Tian and Y.J. Zhao, J. Appl. Phys. **106** (2009) 043707
[9] D.R. Lide, CRC Handbook of Chemistry and Physics, 90th ed., CRC Press, Boca Raton, FL, USA, 2010

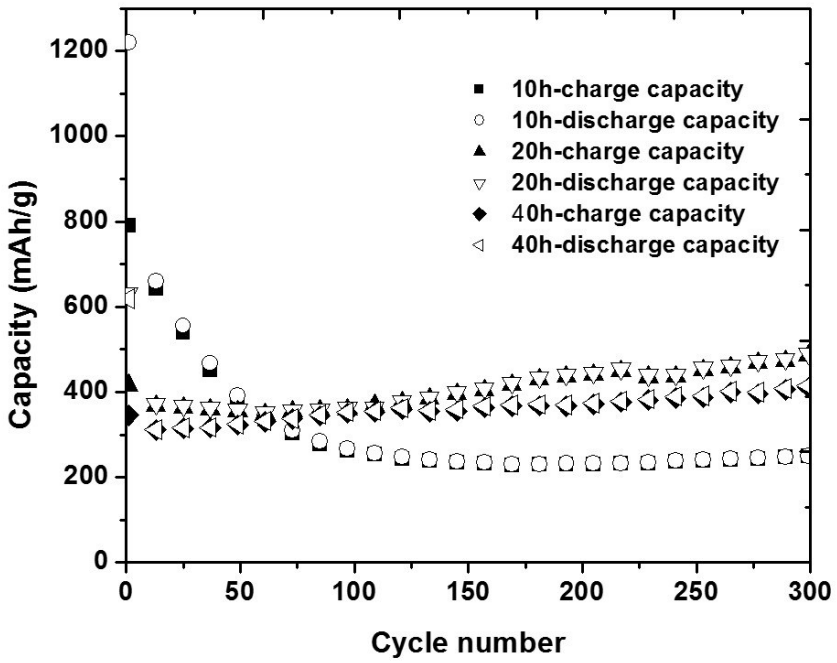

Fig.S1 Comparison of cycle performance for SnO_2/Mn-10h, SnO_2/Mn-20h, SnO_2/Mn-40h composite at a current density of 0.2A/g in the voltage range of 0.01-3V *vs* Li^+/Li, demonstrating that both the shorter (10h) and longer (40h) milling durations induce inferior performance.

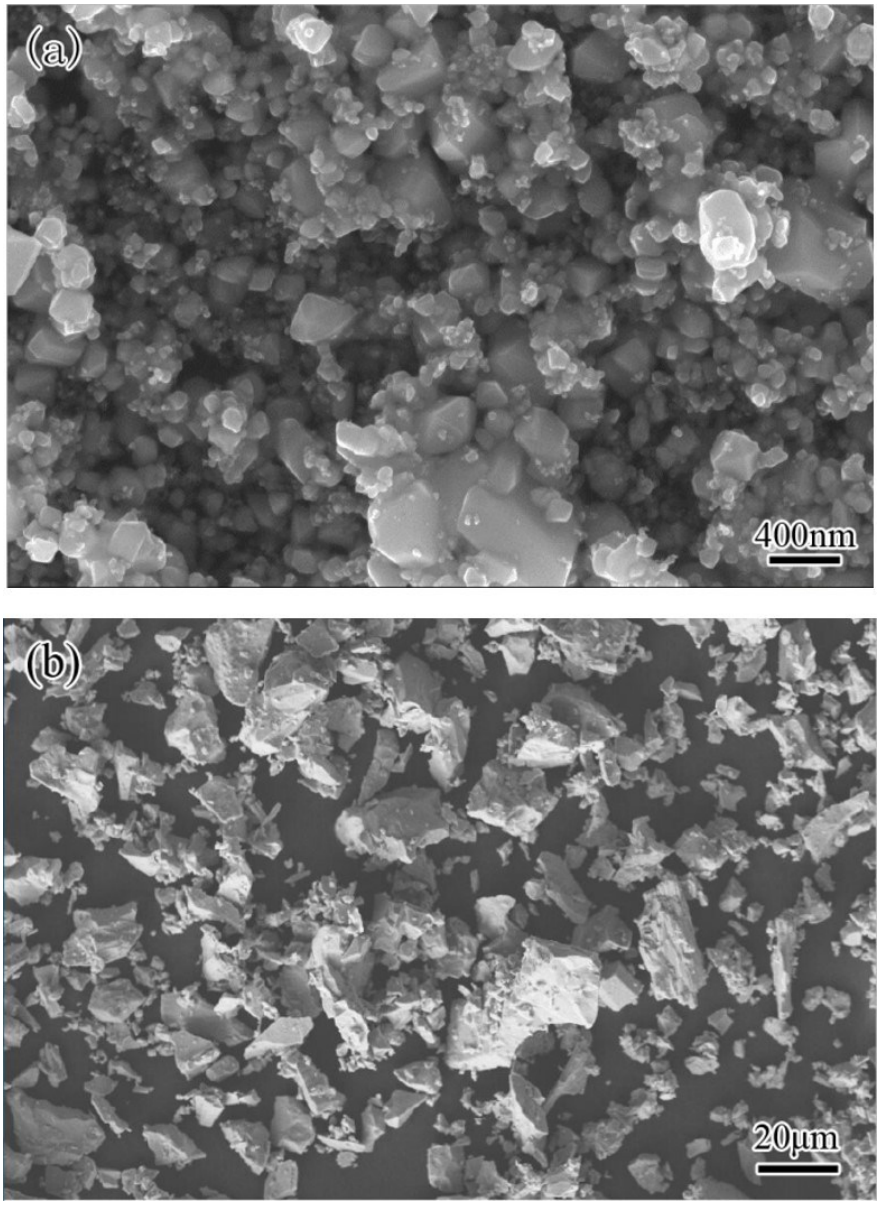

Fig.S2 SEM micrographs of the (a) pristine SnO_2, (b) pristine Mn powders before milling

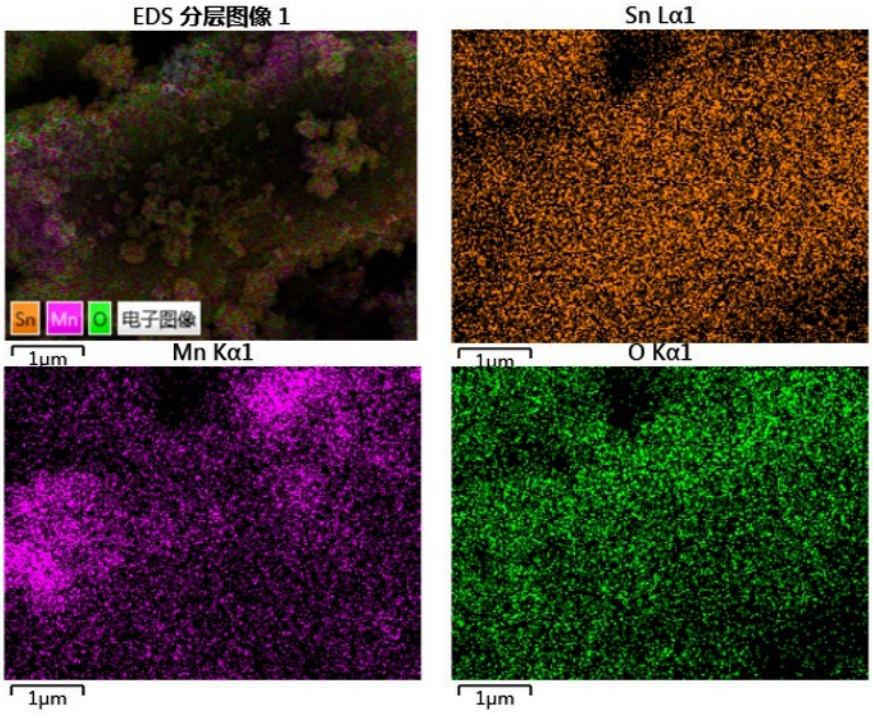

Fig.S3 Element (Sn, Mn, O) mapping of the as-milled SnO_2-30Mn composite

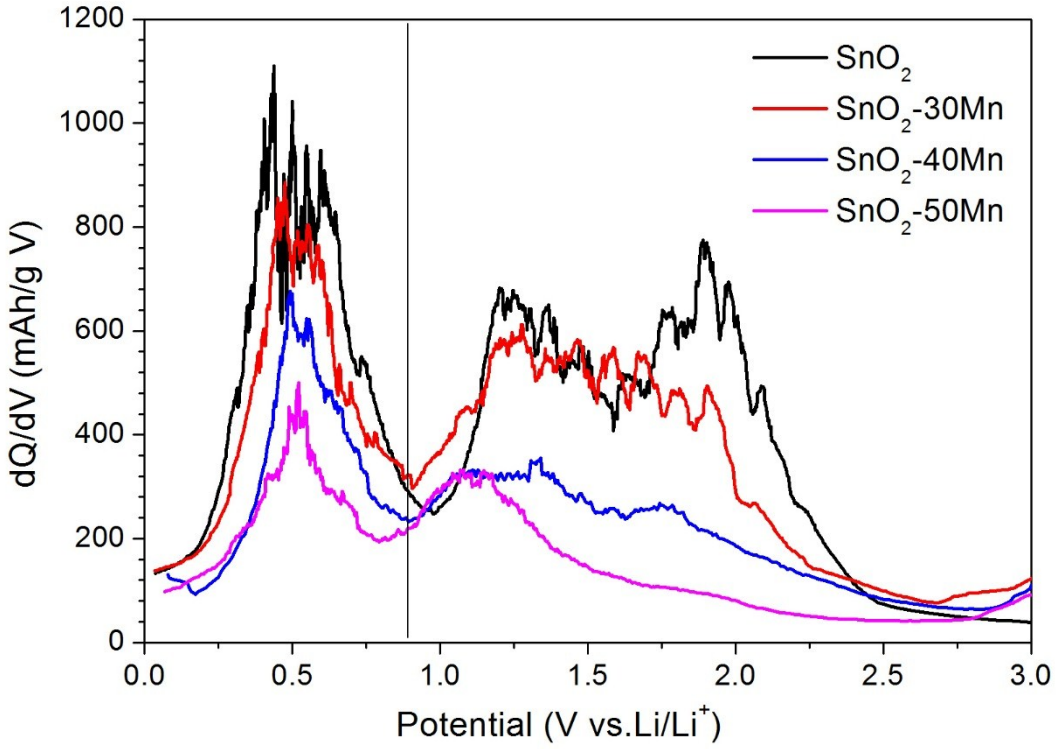

Fig.S4 Differential charge capacity curves for the 1st cycle of the SnO_2, SnO_2-30Mn, SnO_2-40Mn, SnO_2-50Mn electrode, demonstring all the electrode involed dealloying, and reversed conversion reaction during charge.

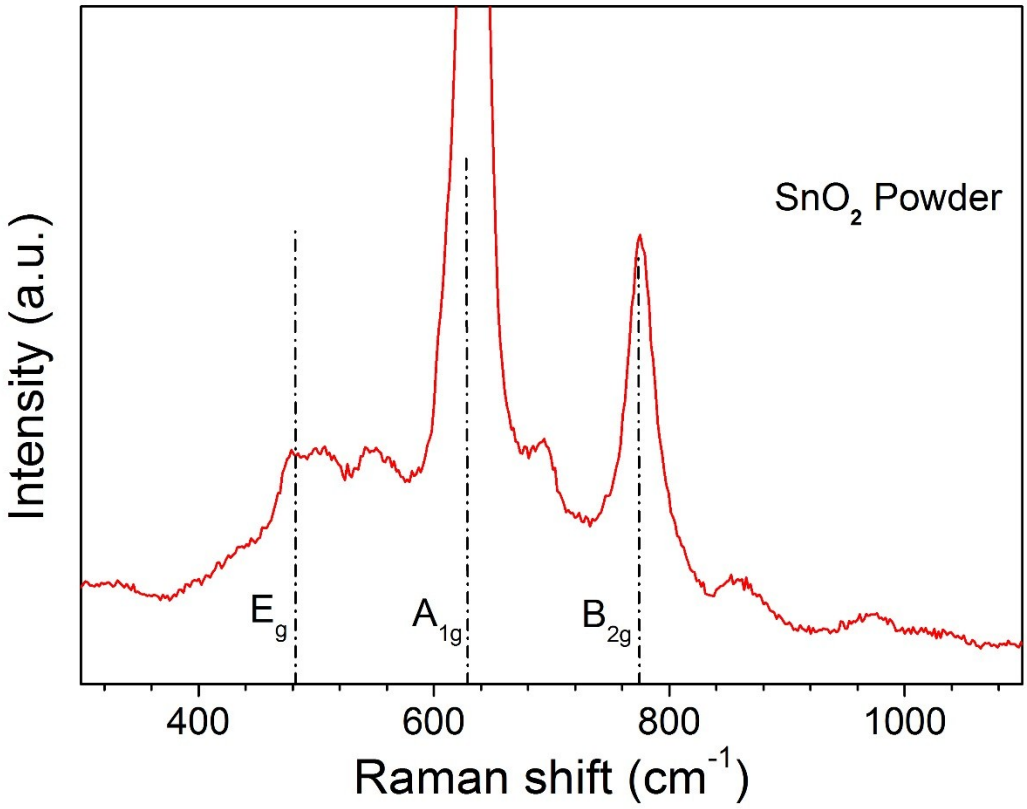

Fig.S5 Raman Spectrum of the un-milled SnO_2 powders.

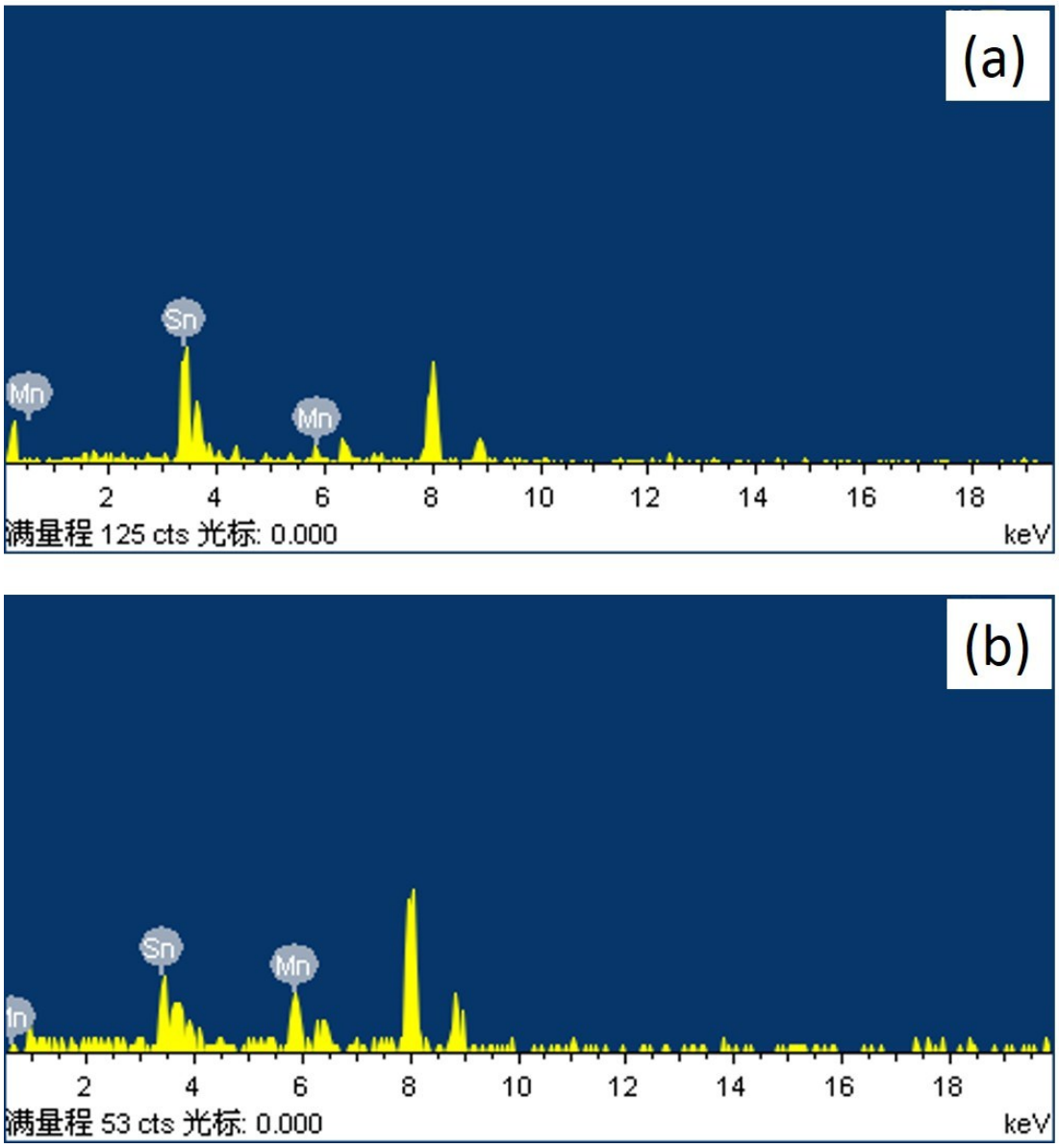

Fig. S6 EDS inspections for the Sn-rich, and Mn-rich regions in the as-milled SnO_2-Mn-graphite composite.

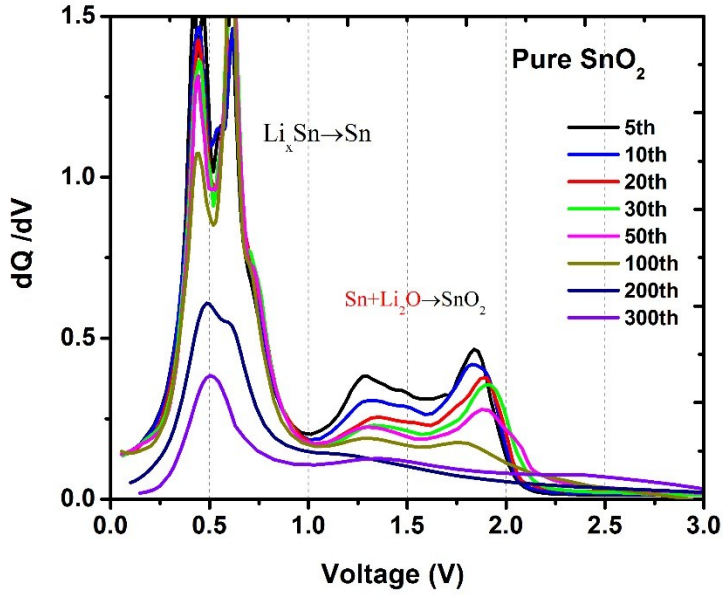

Fig. S7 Differential charge capacity vs. voltage curve of the SnO_2 electrode at the 5^{th}, 10^{th}, 20^{th}, 30^{th}, 50^{th}, 100^{th}, 200^{th} and 300^{th} cycles

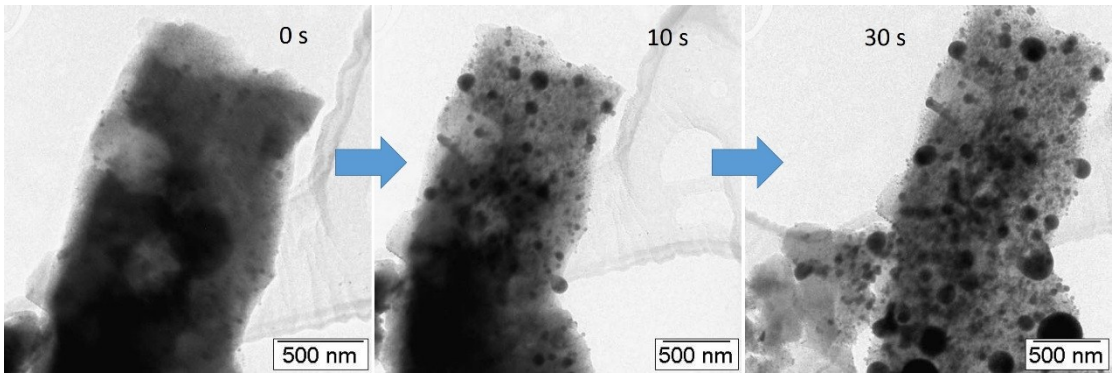

Fig. S8 TEM images showing that the ultrafine Sn nanoparticles are not stable and tending to coarsen and separate out from the carbon matrix at short exposure (several seconds) of electron beam in a partially delithiated SnO_2-G nanocomposite.

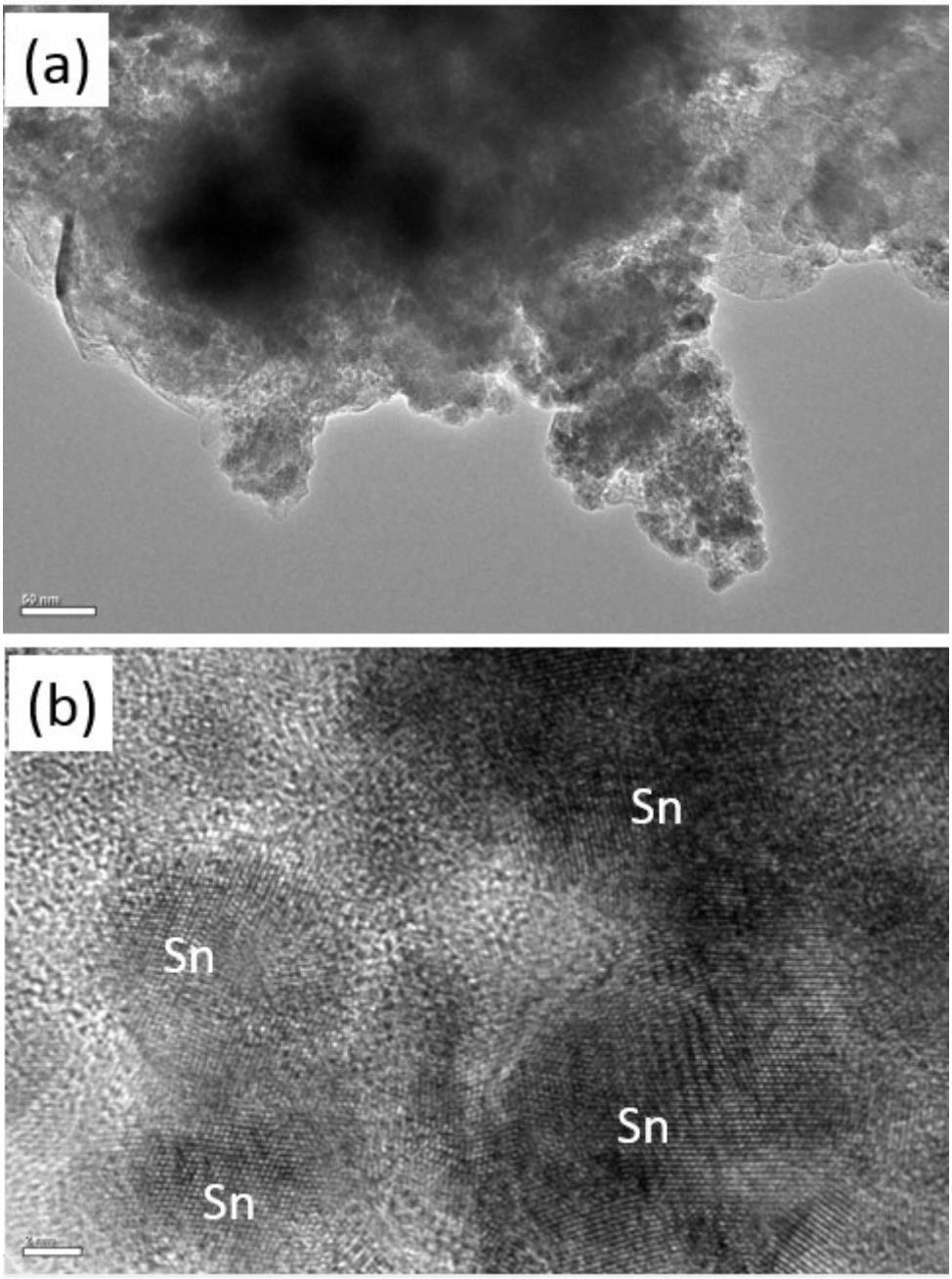

Fig. S9 TEM images of the SnO_2-G electrode after cycling 100 times among 0.01-3.0V. (a) low magnification image, (b) HRTEM image to show the existence of Sn nanocrystals.